Journal of Medicinal Chemistry

Article

A Molecular Combo of Zinc(II) Phthalocyanine and Tamoxifen Derivative for Dual Targeting Photodynamic Therapy and Hormone Therapy

fengling Zhang, Meiru Song, Gan-Kun Yuan, Huannian Ye, Ye Tian, Mingdong Huang, Jinping Xue, Zhihong Zhang, and Jianyong Liu

J. Med. Chem., **Just Accepted Manuscript** • DOI: 10.1021/acs.jmedchem.7b00682 • Publication Date (Web): 12 Jul 2017

Just Accepted

ACS Publications

Journal of Medicinal Chemistry is published by the American Chemical Society. 1155 Sixteenth Street N.W., Washington, DC 20036

A Molecular Combo of Zinc(II) Phthalocyanine and Tamoxifen Derivative for Dual Targeting Photodynamic Therapy and Hormone Therapy

Feng-Ling Zhang, [ξ,ς] *Mei-Ru Song,* [ξ] *Gan-Kun Yuan,* [ξ] *Huan-Nian Ye,* [ξ] *Ye Tian,* [ξ] *Ming-Dong Huang,* [ξ] *Jin-Ping Xue,* [ξ] *Zhi-Hong Zhang,** [ϖ] *and Jian-Yong Liu** [ξ]

[ξ] State Key Laboratory of Photocatalysis on Energy and Environment & Fujian Engineering Research Center of Functional Materials, College of Chemistry, Fuzhou University, 2 Xueyuan Road, University Town, Fuzhou 350108, Fujian, P.R. China

[ϖ] Fuzhou General Hospital of Nanjing Military Command, 156 West Second Ring Road, Fuzhou 350005, Fujian, P.R. China

[ς] College of pharmaceutical science, Zhejiang Chinese Medical University, 548 Binwen Road, Hangzhou, 310053, P. R. China

KEYWORDS

Phthalocyanine, Photodynamic Therapy, Targeting, Combination Treatment, Reactive Oxygen Species

ABSTRACT

The combination of photodynamic therapy and other cancer treatment modalities is a promising strategy to enhance therapeutic efficacy and reduce side effects. In this study, a tamoxifen-zinc(II) phthalocyanine conjugate linked by a triethylene glycol chain has been synthesised and characterised. Having tamoxifen as the targeting moiety, the conjugate shows high specific affinity to MCF-7 breast cancer cells overexpressed estrogen receptors (ER) and tumor tissues, therefore leading to a cytotoxic effect in the dark due to the cytostatic tamoxifen moiety, and a high photocytotoxicity due to the photosensitising phthalocyanine unit against the MCF-7 cancer cells. The high photodynamic activity of the conjugate can be attributed to its high cellular uptake and efficiency in generating intracellular reactive oxygen species. Upon addition of exogenous 17β-estradiol as an ER inhibitor, the cellular uptake and photocytotoxicity of the conjugate are reduced significantly. As shown by confocal microscopy, the conjugate is preferentially localised in the lysosomes of the MCF-7 cells.

INTRODUCTION

Photodynamic therapy (PDT) is a unique invasive treatment for a range of cancers and non-cancerous diseases. It involves the combination of a photosensitiser (PS), light and molecular oxygen ($^3O_2$). Upon irradiation, the excited PS transfers energy to the surrounding $^3O_2$ to generate cytotoxic reactive oxygen species (ROS), especially singlet oxygen ($^1O_2$), which attacks key structural entities within the targeted cells, ultimately resulting in necrosis or apoptosis.[1-3] Although PDT has been extensively studied during recent years and preclinical practices have shown promising results, it is still less commonly used for cancer therapy in clinic. There are two main reasons. First, most of the PSs advanced for PDT lack tumor tissue selectivity, and are also highly taken up by normal tissues, which cause uncomfortable adverse effects, such as skin

photosensitivity and photoallergic reactions.[4] Second, PDT is less effective for huge solid tumors and metastatic tumors. Thus, it is important to develop strategies for enhancing PDT outcomes and reducing its side effects. Two approaches have been extensively used: (1) PS-mediated targeting PDT, which is fulfilled either by making use of nanoparticles modified with target moieties as delivery vehicles for PSs[5-10] or conjugation of PSs to biomacromolecules with targeting function such as antibody[11-13], protein[14-16], peptide[17-21], transferrin[22, 23], aptamer[24, 25] etc. or small molecule targeting ligands such as folic acid[26-28], biotin[29, 30], saccharide[31-33] etc.; (2) mechanism-based combination treatments in which PDT and other therapeutic methods are combined to obtain additive or synergistic effects with advantages, such as enhanced therapeutic efficacy, reduced side effects and retarded drug-resistance problem.[34-52]

Binding of the steroidal hormone 17β-estradiol (E2) to ER is a process essential to normal cell proliferation and differentiation in women.[53] Specific estrogen receptor modulators (SERMs) are an important class of hormone therapy anticancer drugs. They can compete with E2 for binding to ER overexpressed in most of breast cancer cells, conformationally preventing adoption of associated transcription cofactors and subsequently initiating programmed cell death.[54-58] A few of steroid-photosensitiser conjugates have been prepared with a view to improving the targeting ability of PS.[59-61] Tamoxifen, as a SERMs, is regarded to be the first targeted medicine for breast cancer and has achieved considerable success in the treatment of breast tumor.[55-58] Ana Fernandez Gacio et al. reported a tamoxifen-pyropheophorbide conjugate showing specific binding affinity to ER and displaying a strong cell-killing property against MCF-7 breast cancer cells compared with un-conjugated pyropheophorbide upon exposure to red light.[62] The linker between tamoxifen and pyropheophorbide is a long carbon chain (7 carbon atom). The very hydrophobic linker would further render the dissolution of the hydrophobic tamoxifen-

pyropheophorbide conjugate more difficult in biological media. In our current work, an amphiphilic triethylene glycol chain is employed to link tamoxifen and phthalocyanine. It will improve the amphiphilicity and biocompatibility of the conjugate, which may contribute to the cellular uptake leading to an enhanced therapeutic effect.

It is expected that the combination of phthalocyanine and tamoxifen will embrace the advantages of the two different therapeutic mechanisms exhibiting dual targeting photodynamic and hormone therapy for breast cancers. In this paper, we demonstrate the preparation, characterisation, and anticancer activities of such a conjugate, in which a tamoxifen derivative is linked to a zinc(II) phthalocyanine core via a flexible triethylene glycol spacer.

RESULTS AND DISCUSSION

Molecular Design and Synthesis. In conjugate **4**, a zinc(II) phthalocyanine was selected as the photosensitising agent due to its superior photophysical / photochemical properties and high photocytotoxicity. A derivative of tamoxifen, the most widely used SERM, was employed as the targeting and cytostatic component due to its good affinity to ER and subsequently modulation of ER-mediated transcription. The two components were linked by a flexible triethylene glycol chain, which can improve the amphiphilicity and biocompatibility of the conjugate, while maintaining the maximum targeting capacity of tamoxifen. It is expected that the developed tamoxifen-zinc(II) phthalocyanine conjugate can embrace the advantages of the two very different therapeutic mechanisms. Scheme 1 shows the pathway used to prepare conjugate **4**. Firstly, tamoxifen underwent N-desmethylation reaction by addition of α-chloroethyl chloroformate (AcE-Cl) to give intermediate AcE-tamoxifen in CH_2Cl_2, followed by heating the residue in CH_3OH to afford N-desmethylation compound **1**.[63,64] Treatment of this compound

with triethylene glycol monotosylate and K_2CO_3 in CH_3CN produced compound **2**, which was then underwent nucleophilic substitution with 3-nitrophthalonitrile in CH_3CN to give the corresponding phthalonitrile **3**. The "3+1" unsymmetrical phthalocyanine **4** was obtained by the mixed cyclisation of phthalonitrile **3** with an excess of unsubstituted phthalonitrile (9 equiv.) in the presence of $Zn(OAc)_2$ and 1,8-diazabicyclo[5.4.0]undec-7-ene (DBU) in *n*-pentanol. The phthalocyanine could be purified readily by silica gel column chromatography in 9 % yield. All the new compounds were characterised with ^{1}H NMR, HRMS and IR. For comparison, phthalocyanine **M** was prepared as the reference compound (Figure 1).[41]

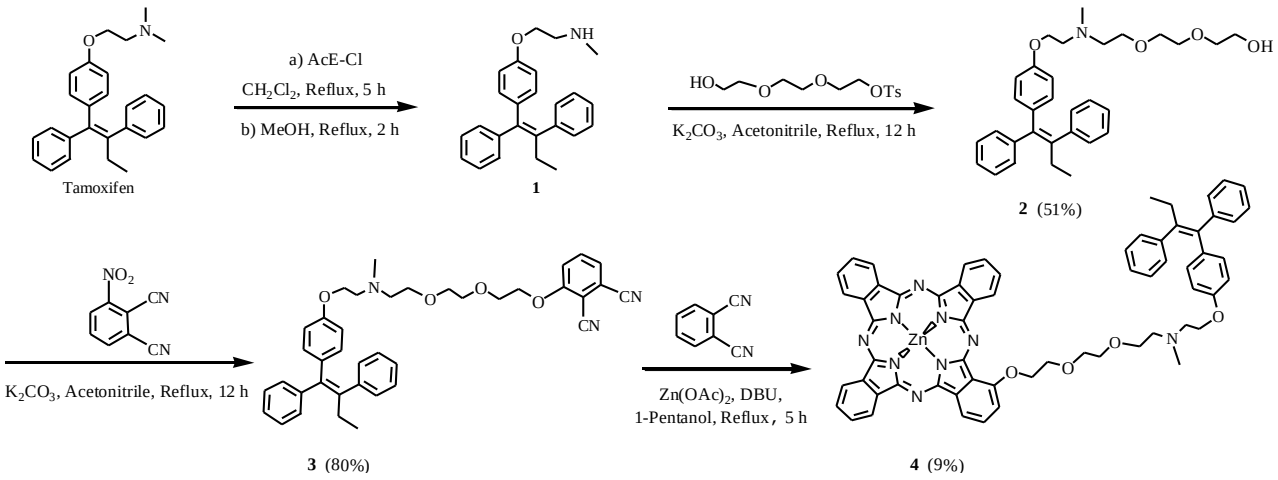

Scheme 1. Synthesis of tamoxifen-zinc(II) phthalocyanine conjugate **4**.

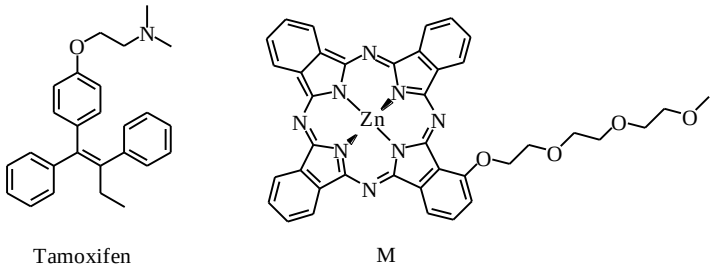

Figure 1. Chemical structures of tamoxifen and reference compound **M**.

Photophysical and Photochemical Properties. The electronic absorption spectrum of conjugate **4** in DMF was recorded (Figure 2). It showed typical features of non-aggregated phthalocyanine displaying an intense and sharp Q band at 678 nm, which strictly followed the Lambert-Beer's law. Upon excitation at 610 nm, conjugate **4** showed a fluorescence emission band at 688 nm with a fluorescence quantum yield (Φ_F) of 0.17 relative to the unsubstituted zinc(II) phthtalocyanine (ZnPc) (Φ_F = 0.28).[65] The electronic absorption and fluorescence data are listed in Table 1.

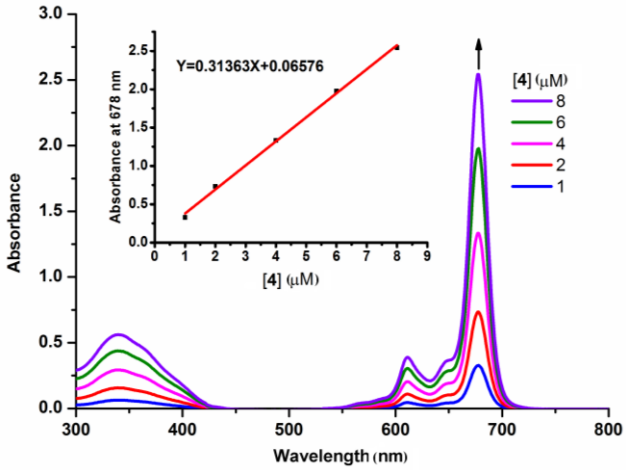

Figure 2. UV/Vis absorption spectra of conjugate **4** in DMF at different concentrations. The inset plots the Q-band absorbance *versus* the concentration of conjugate **4**.

Table 1. Photophysical/photochemical data of **4** and **M** in DMF.

compd	λ_{max} (nm) (logε)	λ_{em} (nm)[a]	Φ_F[b]	Φ_Δ[c]
4	678 (5.50)	688	0.17	0.61
M	677 (5.41)	684	0.26	0.63

[a] Excited at 610 nm. [b] Relative to ZnPc (Φ_F = 0.28 in DMF).[65] [c] Relative to ZnPc (Φ_Δ = 0.56 in DMF).[66]

To evaluate the photosensitising potential, the singlet oxygen quantum yield (Φ_Δ) of conjugate **4** in DMF was determined by a steady-state method using 1, 3-diphenylisobenzofuran (DPBF) as the singlet oxygen scavenger and ZnPc as the standard.[20] The results show that both conjugate **4** and reference **M** are highly efficient singlet oxygen generators (Φ_Δ: 0.61, 0.63 respectively) (Table 1).

***In Vitro* Specificity toward Cancer Cells.** To determine whether the cellular internalisation process of conjugate **4** was mediated by ER, we performed the following uptake competition experiments using 17β-estradiol as an ER inhibitor. ER+ MCF-7 breast cancer cells were initially incubated with 17β-estradiol (0, 25, 50 μM) for 30 h, and subsequently with conjugate **4** or reference **M** (0.5 μM) for 24 h. Images from the cells (Figure 3A) by Olympus FV 1000 confocal laser scanning microscope indicated that addition of exogenous 17β-estradiol significantly inhibited the uptake of conjugate **4** by the MCF-7 cancer cells and the inhibition was dependent on the concentration of exogenous 17β-estradiol. Intracellular fluorecence measurements quantitatively showed that the uptake of conjugate **4** by MCF-7 cancer cells decreased with the increasing concentrations of 17β-estradiol (from 0 to 50 μM), and the uptake was suppressed almost up to 80% at 17β-estradiol concentration of 50 μM (Figure 3B). The competitive responses are in agreement with previous report indicating 1-2 orders of magnitude greater ER binding ability for 17β-estradiol *versus* tamoxifen.[67] By contrast, the uptake of phthalocyanine **M** by the MCF-7 cancer cells did not change by addition of exogenous 17β-estradiol (Figures 3A and 3B). The comparable uptake experiments have also been performed between MCF-7 cells with high expression of ER (ER+) and MDA-MB-231 cells having low

expression of ER (ER-). As expected, the MCF-7 cells show a much higher uptake to conjugate **4** than MDA-MB-231 cells (Figure 3D).

Photocytotoxicity of conjugate **4** toward MCF-7 cancer cells in the prescence of exogenous 17β-estradiol was also investigated. MCF-7 cancer cells were firstly incubated with various concentrations of 17β-estradiol for 30 h, and subsequently with conjugate **4** or reference **M** (0.05 μM) for 24 h. Then the cells were exposure to red light (λ = 670 nm, 80 $mW \cdot cm^{-2}$, 1.5 $J \cdot cm^{-2}$). As shown in Figure 3C, the photodynamic activity of conjugate **4** decreased with the increasing concentrations of 17β-estradiol (from 0 to 50 μM), and about 45% of cytotoxcity was suppressed at 17β-estradiol concentration of 50 μM ($P < 0.01$). By contrast, the photocytotoxicity of phthalocyanine **M** was independent on the presence of 17β-estradiol. The results are in accord with the cellular uptake competition experiments. The ER expression-dependent uptake and photodynamic activity observed here clearly suggest that, as expected, conjugate **4** has obvious receptor-dependent targeting ability toward ER+ cancer cells. In fact, except the experiment program we used in this manuscript, there would be a better way for the "competition study" by adding the conjugate at the same time mixed with the increasing concentrations of 17β-estradiol.

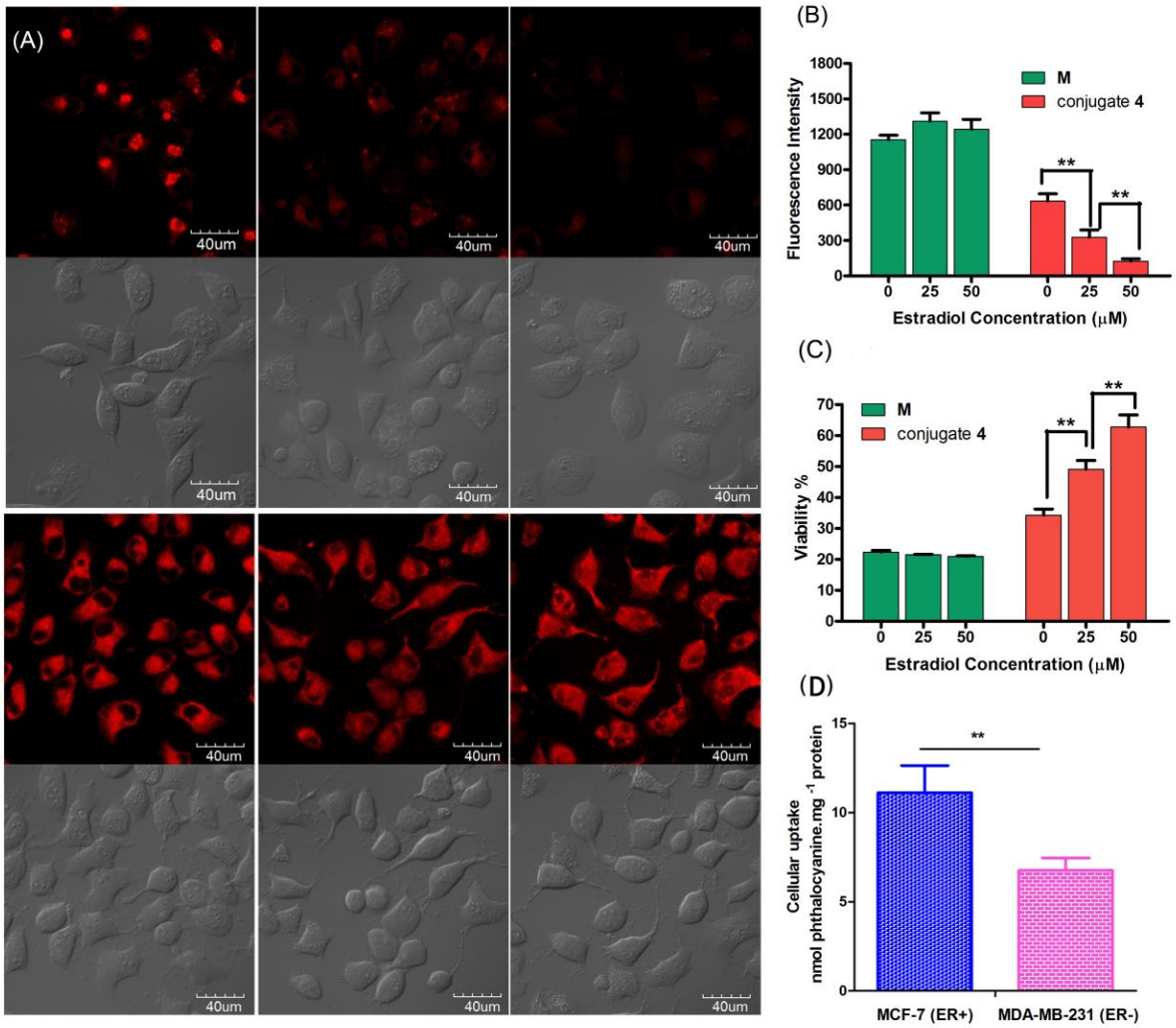

Figure 3. Cellular uptake and cell viability competition experiments. (A) Confocal images of MCF-7 breast cancer cells treated with 0.5 μM conjugate **4** (upper two row) or reference **M** (lower two row), in the presence of 17β-estradiol (from left to right: 0, 25, 50 μM). (B) The histogram statistics of phthalocyanines' intracellular fluorescence from confocal images (mean ± SD, ca. 10 cells). (C) Photocytotoxic effects of conjugate **4** and reference **M** (0.05 μM) toward MCF-7 cancer cells in the prescence of 17β-estradiol (0, 25, 50 μM). Data are expressed as mean ± SD of three independent experiments. Statistical significant ** ($P < 0.01$). (D) Comparable uptake of conjugate **4** by MCF-7 and MDA-MB-231 cells.

***In Vivo* Specificity toward Tumor Tissues.** To further confirm the specificity of conjugate **4** to ER+ tumor tissues, the *in vivo* three-dimensional fluorescence imaging was performed by *in vivo* fluorescence molecular tomography (FMT) using the FMT^{TM} 2500 system (PerkinElmer Inc.) excited at 680 nm and detected at 690-740 nm. Conjugate **4** and reference **M** were injected into Balb/c nude mice bearing MCF-7 tumor through the tail vein. As shown in Figures 4A and 4B, at 48 h after administration, the total amount of conjugate **4** in tumor was visibly higher than that of **M**; the tumor/normal tissue mole ratio of conjugate **4** was actually about 5, while it was only 1.8 for **M**, which can attribute to the slight passive tumor selectivity of phthalocyanine-based photosensitiser. At 96 h after administration, the tumors were striped from the mice and the fluorescence imaging was also performed by FMT (Figure 4C). It could be seen that the fluorescence intensity of conjugate **4** in tumor was obvious higher than in normal tissue, and also much higher than **M** in tumor. Figures 4D and 4E showed the optic slices of conjugate **4** and reference **M** in the centre of the tumors at 48 h, the fluorescence intensity of conjugate **4** in tumor centre was obvious higher than that of **M**, which is in accord well with the results observed in Figures 4A and 4B. At different time points (24 h, 48 h, 72 h, and 96 h after injection), the average concentrations of photosensitisers in the tumor and normal tissue were quantitated by FMT. As shown in Figure 4F, conjugate **4** exhibited an increasing tumor/normal tissue mole ratio in 48 hours and then gradually decreased. However, the tumor/normal mole ratio of compound **M** showed no obvious changes along with time. All the results indicate that conjugate **4** is highly specific affinity to ER+ tumor over normal tissues.

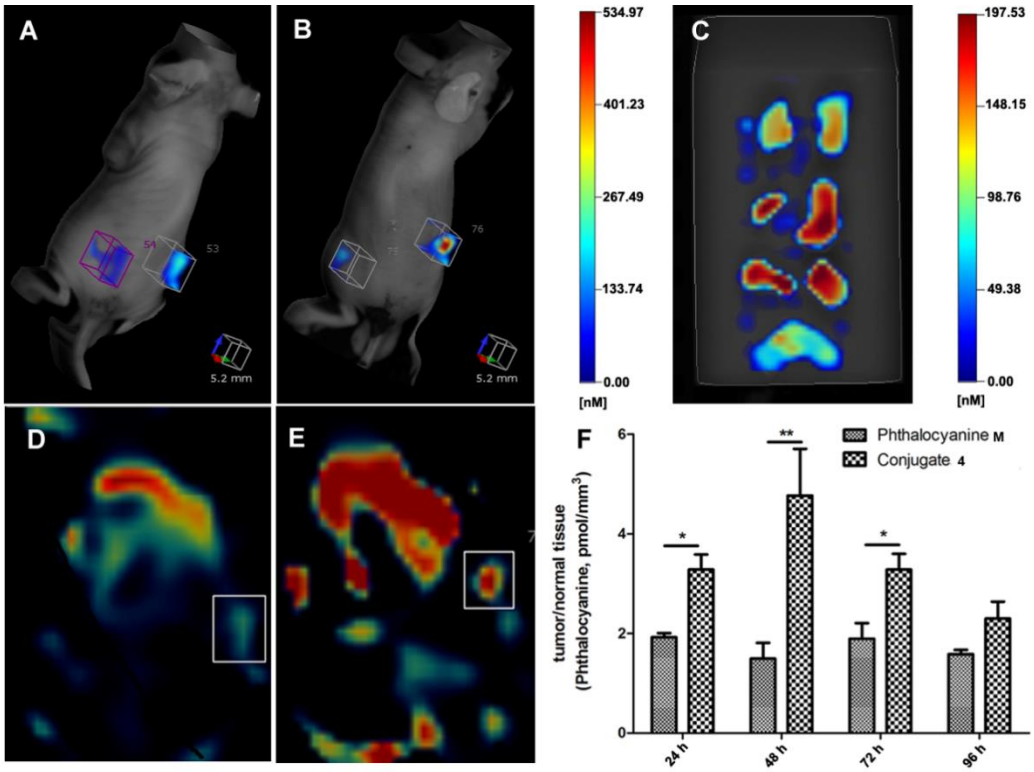

Figure 4. In vivo specificity study using nude mice with subcutaneous MCF-7 tumors. Three-dimensional fluorescence signal based on FMT, at 48 h after administration with (A) **M** and (B) **4**. (C) FMT imaging of striped tumors from the mice treated with **M** (on the top row) and **4** (on the two rows in the middle), and skin of the mice treated with **4** (on the bottom row) at 96 h after injection. Transverse slice of FMT reconstruction overlaid on centrial axle of nude mice administrated by (D) **M** and (E) **4** at 48 h after injection. (F) comparison of the average value of time-dependent tumor/normal tissue biodistribution ratio of **4** and **M**. Statistical significant ** ($P < 0.01$), * ($P < 0.05$).

***In Vitro* Photodynamic Activities.** The *in vitro* photodynamic activities of phthalocyanines **4** and **M** against MCF-7 cancer cells were investigated. The corresponding dose-dependent survival curves are shown in Figure 5A and IC_{50} values are summarised in Table 2. It can be seen that both compounds were essentially noncytotoxic in the absence of light up to 1 μM. In

contrast, they exhibited significantly high photocytotoxicities toward MCF-7 cancer cells with IC_{50} values as low as 13.80 ±1.94 and 11.27 ±0.77 nM (Figure 5A, Table 2) under a rather low light dose (λ = 670 nm, 80 mW cm^{-2}, 1.5 J cm^{-2}). The photodynamic activity of conjugate **4** was also evaluated using calcein AM which can be well retained within live cells, conversing the virtually nonfluorescent cell-permeant calcein AM to the intensely fluorescent calcein (ex/em ~488 nm/~520-540 nm).[68] Figure 5B shows the cytotoxic effects of conjugate **4** towards MCF-7 cancer cells in the presence of different drug concentration (0.005, 0.05, 0.5 μM) under irradiation. It showed obviously dose-dependent antiproliferative properties. All the cells were stained by calcein AM and did not show obvious morphological changes under a rather low drug concentration (0.005 μM), indicating conjugate **4** is extremely low cytotoxic towards MCF-7 cancer cells under this condition. At 0.05 μM, about one-third of the cells were stained by calcein AM and two-third of the cells had morphological changes, shrinkage, size reduction, and turned round. However, when the drug concentration arrived at 0.5 μM, no cells were stained by calcein AM and all of the cells completely lost their shapes. The results clearly show that conjugate **4** well maintains the photodynamic activity of phthalocyanine core.

Due to the large-conjugated structure, phthalocyanine derivatives tend to aggregate, as a result, their photodynamic activities are greatly reduced or even disappeared.[69] To account for the *in vitro* photodynamic activities, the aggregation behavior of phthalocyanines **4** and **M**, formulated with Cremophor EL in the DMEM culture medium, was examined by UV/Vis absorption spectra. As shown in Figure S1 in Electronic Supporting Information, both phthalocyanines showed a relatively sharp and intense Q-band suggesting that they were not significantly aggregated under these conditions, which seems to be in accord with their high photocytotoxicities.

The excitation of the photosensitiser results in the generation of ROS, which is thought to be the main mediator of cellular death induced by PDT. Here, the intracellular ROS production of **4** was also evaluated by using 2′, 7′-dichlorodihydrofluorescein diacetate (DCFH-DA) as the indicator.[66] DCFH-DA was initially nonfluorescent, its oxidised product (DCF) by ROS could emit a green fluorescence. As shown in Figure 5C, conjugate **4** can sensitise the formation of ROS under irradiation and its ROS production efficiency showed an increased tendency along with the dye concentrations which is well in accord with its dose-dependent antiproliferative properties.

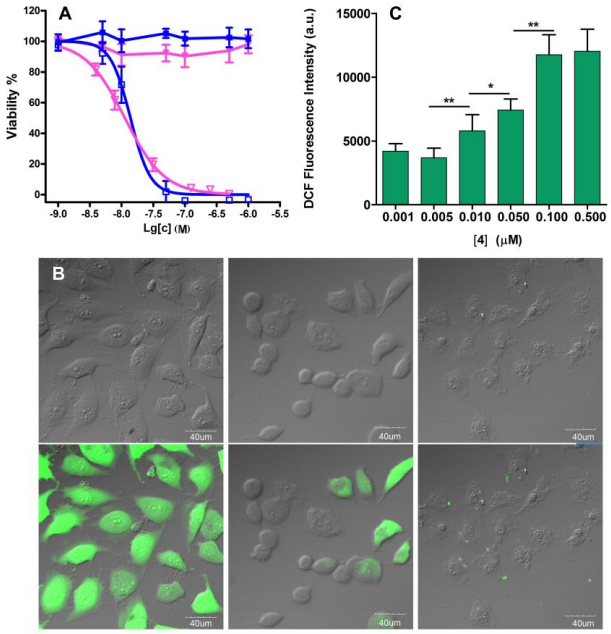

Figure 5. (A) Cytotoxic effects of conjugate **4** (squares) and reference **M** (triangles) towards MCF-7 cancer cells in the presence (open symbols) and absence (close symbols) of light (λ=670 nm, 80 mW·cm^{-2}, 1.5 J·cm^{-2}). Data are expressed as mean ± SD of three independent experiments, each performed in sextuple. (B) Confocal Images of cells stained with calcein AM after administration with different concentration of conjugate **4** (0.005, 0.05, 0.5 μM, from left to right) upon illumination. (C) The concentration-dependent intracellular ROS production of

conjugates **4**. Data are expressed as mean ± SD of three independent experiments. Statistical significant * ($P < 0.05$), **($P < 0.01$).

Table 2. IC_{50} values for conjugate **4** and reference **M** against MCF-7 cells

compd	IC_{50}[a] (nM)
4	13.80±1.94
M	11.27±0.77

[a] in the presence of light (λ=670 nm, 80 mW cm^{-2}, 1.5 J cm^{-2}), Data are expressed as mean value±SD of three independent experiments, each performed in sextuple.

***In Vitro* Antiproliferation Activities in Dark.** To confirm the hormone treatment of the tamoxifen–zinc(II) phthalocyanine conjugate, the antiproliferative activities of conjugate **4**, reference **M**, and tamoxifen were examined in dark (Figure 6). It can be seen that tamoxifen showed substantial cytotoxicity toward MCF cancer cells with an IC_{50} value of 21.05 μM, phthalocyanine **M** only exhibited about 25% cell killing effect at this concentration. However, conjugate **4** showed a relatively higher cytotoxicity (about 50% cell killing effect) at a lower concentration (12.5 μM), which can be attributed to the additional antitumor effect of the tamoxifen moiety.

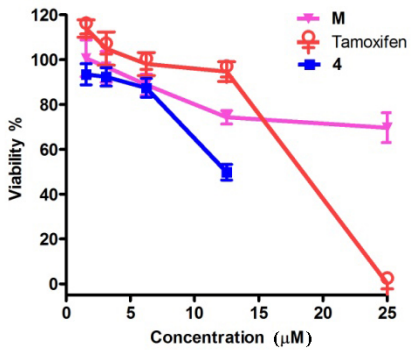

Figure 6. Cytotoxic effects of conjugate **4**, reference **M** and tamoxifen towards MCF-7 cancer cells in the absence of light. Data are expressed as mean ± SD of three independent experiments, each performed in sextuple.

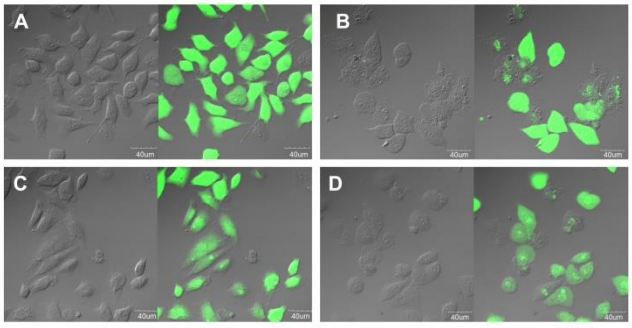

Figure 7. Confocal images of cells stained with calcein AM after administration with (A) solvent (control), (B) conjugate **4** (12.5 μM), (C) phthalocyanine **M** (12.5 μM) and (D) tamoxifen (12.5 μM) in the absence of light.

Antiproliferative activities of conjugate **4**, reference **M**, and tamoxifen were also studied using calcein AM assay. Figure 7 shows their cytotoxic effects towards MCF-7 cancer cells at a drug concentration of 12.5 μM in dark. All the cells were stained by calcein AM and did not show morphological changes in the absence of drug (Figure 7A). When treated with tamoxifen, most of the cells had obvious morphological changes, shrinkage, size reduction and turned round

indicating the cells were in a state of apoptosis (Figure 7D). Administrated with **M**, only a small amount of cells died or had morphological changes indicating its low antiproliferative activity (Figure 7C). However, exposed to conjugate **4**, more than 50% cells died and most of cells had morphological changes, which suggested it had higher antiproliferative activity (Figure 7B). The results clearly showed that conjugate **4** exhibited an enhanced antiproliferative activity compared with reference **M**. The additional cytotoxcity was due to tamoxifen moiety. In addition, conjugate **4** showed high specificity towards cancer cells with high expression of ER, and well maintained the photodynamic activity of phthalocyanine core. All the results indicated that the two antitumor components in conjugate **4** exhibited the combined anticancer effects.

As a control, the photocytotoxicity of an equimolar mixture of **M** and tamoxifen has been studied and compared with that of conjugate **4**. It can be seen in Figure S2 that its photocytotoxicity is comparable with that of **4**. It means that conjugate **4** may only act in a combined manner, not a synergetic manner. Of course, it is more likely that a synergetic effect occurs in conjugate **4**, but is not observed. This may be because the cytotoxicity of phthalocyanine moiety is much higher than that of tamoxifen unit in **4** (IC_{50} = 13 nM vs 21 μM, 3 orders of magnitude difference). In this case, it is very difficult to show the synergetic effect by a control experiment. Anyway, conjugate **4** shows a combined photodynamic and hormone therapy. It exhibits high selectivity to cancer cells, which leads to a relatively low side effect. However, an equimolar mixture of **M** and tamoxifen does not have the advantages.

Subcellular Localization. In addition, the subcellular localisation of conjugate **4** was also incubated with the conjugate **4** at 10 μM in the DMEM culture medium for 24 h, and then stained with Lyso-Tracker DND 26 or Mito-Tracker Green FM (for 30 min) or DAPI (for 10

min), which are specific dyes for lysosomes, mitochondria, and nucleus respectively. As shown in Figure 8A, the fluorescence caused by the LysoTracker (excited at 488 nm, monitored at 510−570 nm) can superimpose well with the fluorescence caused by conjugate **4** (excited at 633 nm, monitored at 650−750 nm). The very similar fluorescence intensity line profiles of conjugate **4** (red) and LysoTracker (blue) traced along the white line in the merged images also confirmed that conjugate can well target the lysosomes of the cells (Figure 8B). By contrast, the fluorescence images of conjugate could not be merged well with that of MitoTracker (excited at 488 nm, monitored at 510-570 nm) and DAPI (excited at 405 nm, monitored at 425−475 nm) indicating conjugate **4** is not localised in the mitochondria and nucleus of the cells. This may be explained by the protonation of conjugate **4** bearing tamoxifen caused by lower lysosomal pH. By this way, the conjugate **4** becomes more water-soluble, it would be detained in the lysosomes due to greater difficulty in crossing the lysosomal membrane.

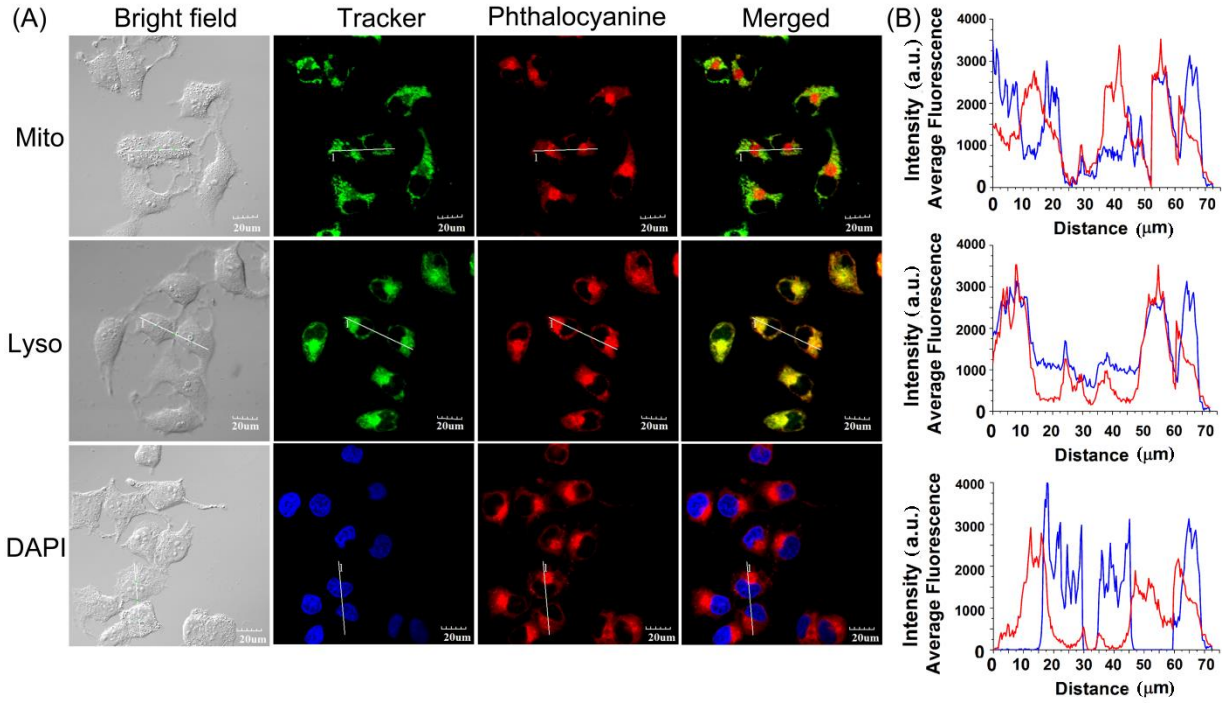

Figure 8. (A) Confocal fluorescence images of MCF-7 cancer cells treated with conjugate **4** (column 3) and Mito-Tracker, Lyso-tracker, or DAPI (column 2). (B) Fluorescence intensity profiles of conjugate **4** (red line) and Tracker (blue line) traced along the white lines in the merged images.

CONCLUSIONS

In summary, we have reported the synthesis, characterisation and anticancer activities a novel zinc(II) phthalocyanine derivative substituted with a small molecule target-based cancer therapy drug tamoxifen via a flexible triethylene glycol chain. As expected, the conjugate showed high specific affinity to MCF-7 breast cancer cells and tumor tissues, therefore resulting in a heavy cytotoxic effect in the dark due to the cytostatic tamoxifen moiety, and a high photocytotoxicity due to the photosensitising phthalocyanine core against the MCF-7 cancer cells. Competition experiments indicated that the cellular uptake and *in vitro* photodynamic activity of this conjugate was substantially inhibited upon addition of exogenous 17β-estradiol. The overall

results show that this tamoxifen-zinc(II) phthalocyanine conjugate is a highly promising photohormonetherapy (PHT) agent for dual targeting photodynamic and hormone therapy to breast cancers. The detailed mechanism of the PDT action of this conjugate and its *in vivo* PDT efficacy are under investigation.

EXPERIMENTAL SECTION

General. All the reactions were performed under an atmosphere of nitrogen. *n*-Pentanol was distilled from sodium. All other solvents and reagents were of reagent grade and used as received. ^{1}H NMR spectra were recorded on AVANCE III 400 (^{1}H, 400 MHz) spectrometer in $CDCl_3$ or DMSO-d_6. Chemical shifts were expressed in ppm relative to TMS (0 ppm). HRMS analyses were carried on an ion trap mass spectrometry DECAX-30000 LCQ Deca XP mass spectrometer. IR spectra were measured on a Perkin-Elmer SP2000. Electronic adsorption spectra were measured on a Beijing PuXi Tu-1901 spectrometer. Fluorescence spectra were obtained on a Varian Cary eclipse spectrometer. Subcellular location was carried on Olympus FV1000 confocal laser scanning microscope; *In vivo* fluorescence imaging was recorded on PerkinElmer Fluorescence Molecular Tomography (FMTTM 2500LX). The purity of all new compounds was determined by HPLC analysis and was found to be ≥ 95%.

Synthesis and Characterisation.

Compound 2. A mixture of compound **1** (3.57 g, 10.0 mmol), triethylene glycol monotosylate (3.65 g, 12.0 mmol) and K_2CO_3 (5.53 g, 40.0 mmol) in acetonitrile (40 mL) was stirred at 85 ℃ under an atmosphere of nitrogen for 12 h. The volatiles were removed in vacuo. Then the residue was mixed with water (50 mL) and extracted with CH_2Cl_2 (50 mL×3). The combined organic

extracts was dried and then purified by silica gel column chromatography using CH_2Cl_2/CH_3OH (30:1 v/v) as the eluent to give compound **2** as a yellow viscous liquid (2.50 g, 51%). ^{1}H NMR (400 MHz, $CDCl_3$): δ = 0.93 (t, *J* = 7.6 Hz, 3 H, CH_3), 2.38 (s, 3 H, CH_3), 2.43-2.49 (m, 2 H, CH_2), 2.72 (br s, 2 H, CH_2), 2.84 (br s, 2 H, CH_2), 3.58-3.62 (m, 6 H, CH_2), 3.64-3.67 (m, 2 H, CH_2), 3.69-3.71 (m, 2 H, CH_2), 3.97 (t, *J* = 6.0 Hz, 2 H, CH_2), 6.55 (d, *J* = 8.8 Hz, 2 H, Ar-H), 6.77 (m, *J* = 9.2 Hz, 2 H, Ar-H), 7.10-7.13 (m, 3 H, Ar-H), 7.16-7.20 (m, 2 H, Ar-H), 7.24-7.26 (m, 2 H, Ar-H), 7.27-7.29 (m, 1 H, Ar-H), 7.33-7.37 ppm (m, 2 H, Ar-H); ^{13}C NMR (100.6 MHz, DMSO-d_6): δ = 156.57, 143.41, 141.91, 140.80, 138.05, 134.97, 131.44, 129.48, 129.06, 128.41, 128.06, 126.79, 126.31, 113.57, 72.44, 69.86, 69.79, 68.80, 65.74, 60.33, 56.76, 56.17, 42.95, 28.63, 13.47; HRMS (ESI): *m/z* calcd for $C_{31}H_{39}NO_4$ $[M + H]^+$, 490.2952; found: 490.2989; IR: υ_{as} (-CH_3,) 2967, 2925, 2869, υ(Ar) 1604, 1513, 1464, 1443, υ_{as} (C-O-C) 1240, 1171, 1113, 1066 cm^{-1}.

Phthalonitrile 3. A mixture of compound **2** (4.90 g, 10.0 mmol), 2,3-dicyano-1-nitrobenzene (2.08 g, 12.0 mmol) and K_2CO_3 (5.53 g, 40.0 mmol) in acetonitrile (30 mL) was stirred at 85 °C under an atmosphere of nitrogen for 12 h. Acetonitrile were evaporated under reduced pressure, and then the residue was extracted with CH_2Cl_2. The combined organic extracts were dried in vacuo. The residue was purified by silica gel column chromatography using CH_2Cl_2/CH_3OH (50:1 v/v) as the eluent to give compound **3** as a brown viscous liquid (4.90 g, 80%). ^{1}H NMR (400 MHz, $CDCl_3$): δ = 0.94 (t, *J* = 7.6 Hz, 3 H, CH_3), 2.39 (s, 3 H, CH_3), 2.47 (m, 2 H, CH_2), 2.72 (vt, *J* = 6.0 Hz, 2 H, CH_2), 2.84 (vt, *J* = 6.0 Hz, 2 H, CH_2), 3.60-3.64 (m, 4 H, CH_2), 3.73-3.75 (m, 2 H, CH_2), 3.91 (vt, *J* = 4.8 Hz, 2 H, CH_2), 3.96 (vt, *J* = 5.6 Hz, 2 H, CH_2), 4.28 (vt, *J* = 4.4 Hz, 2 H, CH_2), 6.55 (d, *J* = 8.8 Hz, 2 H, Ar-H), 6.78 (d, *J* = 8.4 Hz, 2 H, Ar-H), 7.11-7.15 (m, 3 H, Ar-H), 7.17-7.21 (m, 2 H, Ar-H), 7.25-7.27 (m, 3 H, Ar-H), 7.27-7.30 (m, 1 H, Ar-H), 7.35-

7.38 (m, 3 H, Ar-H), 7.59 ppm (vt, J = 8.8 Hz, 1 H, Ar-H); ^{13}C NMR (100.6 MHz, DMSO-d_6): δ = 161.06, 156.50, 143.35, 141.86, 140.74, 137.99, 135.81, 134.91, 131.37, 129.42, 129.00, 128.34, 127.99, 126.73, 126.24, 125.87, 118.89, 115.87, 115.45, 113.73, 113.50, 103.04, 70.14, 69.74, 69.53, 68.73, 68.54, 65.67, 56.69, 56.08, 42.90, 28.58, 13.41; HRMS (ESI): *m/z* calcd for $C_{39}H_{41}N_3O_4$ $[M + H]^+$, 616.3170; found: 616.3133; IR: υ (-CN) 2229, υ_{as} (-CH_3) 2923, 2880, υ_s (-CH_3) 1391, υ(Ar) 1621, 1581, 1505, 1451, 1427, υ_{as} (C-O-C) 1293, 1241, 1206, 1123, 1065 cm^{-1}.

Conjugate 4. To a mixture of phthalonitrile **3** (0.25 g, 0.41 mmol), 1,2-dicyanobenzene (0.47 g, 3.7 mmol) and $Zn(OAc)_2$ (0.38 g, 2.1 mmol) in 12 mL *n*-pentanol was added 0.7 mL DBU. The resulting solution was stirred at 150 °C under an atmosphere of nitrogen for 5 h. The volatiles were removed in vacuo. The residue was purified by silica gel column chromatography using CH_2Cl_2/CH_3OH (30:1 v/v) as the eluent to give phthalocyanine **4** as a blue solid (0.04 g, 9%). ^{1}H NMR (400 MHz, DMSO-d_6): δ = 0.66 (t, J = 7.2 Hz, 3 H, CH_3), 2.08 (s, 3 H, CH_3), 2.13-2.19 (m, 2 H, CH_2), 2.46 (br s, 4 H, CH_2), 3.47 (vt, J = 5.2 Hz, 2 H, CH_2), 3.56 (vt, J = 5.2 Hz, 2 H, CH_2), 3.68 (vt, J = 4.4 Hz, 2 H, CH_2), 4.02 (vt, J = 4.4 Hz, 2 H, CH_2), 4.34 (br s, 2 H, CH_2), 4.78 (br s, 2 H, CH_2), 6.21 (d, J = 8.4 Hz, 2 H, Ar-H), 6.35 (d, J = 8.4 Hz, 2 H, Ar-H), 6.83 (d, J = 6.4 Hz, 2 H, Ar-H), 6.93 (d, J = 7.2 Hz, 2 H, Ar-H), 6.97-7.00 (m, 3 H, Ar-H), 7.15-7.25 (m, 3 H, Ar-H), 7.57 (d, J = 8.0 Hz, 1 H, Pc-H_β), 7.96 (t, J = 7.6 Hz, 1 H, Pc-H_β), 8.13-8.19 (m, 6 H, Pc-H_β), 8.77 (d, J = 7.2 Hz, 1 H, Pc-H_α), 9.13 (d, J = 6.4 Hz, 1 H, Pc-H_α), 9.22-9.27 ppm (m, 5 H, Pc-H_α); ^{13}C NMR (100.6 MHz, DMSO-d_6 with a drop of pyridine-d_5): δ = 156.11, 155.54, 152.74, 152.70, 152.59, 152.56, 152.53, 152.45, 152.37, 143.18, 141.71, 140.69, 140.13, 138.26, 138.01, 137.97, 137.91, 137.87, 137.84, 134.85, 131.08, 130.57, 129.29, 129.18, 129.05, 128.81, 128.24, 127.84, 126.61, 126.10, 124.67, 122.37, 122.31, 122.21, 114.88, 113.33, 113.24, 70.61,

70.03, 70.00, 68.81, 68.25, 65.03, 56.42, 55.72, 42.55, 28.44, 13.29; HRMS (ESI): *m/z* calcd for $C_{63}H_{53}N_9O_4Zn$ $[M + H]^+$, 1064.3585; found: 1064.3591; IR: υ(Pc) 1599, 1484, 1447, υ_{as} (C-N) 1325, υ(Ar-O-R) 1271, υ_{as} (C-O-C) 1174, 1113, 1078, 1049 cm^{-1}.

Photophyscial and Photochemical Studies. Fluorescence quantum yields (Φ_F) were measured according to the equation: $\Phi_F(\text{sample}) = (F_{\text{sample}} / F_{\text{ref}}) (A_{\text{ref}} / A_{\text{sample}}) (\eta_{\text{sample}}^2 / \eta_{\text{ref}}^2) \Phi_F(\text{ref})$, where F, A, and η are the integrated fluorescence area (λ_{ex} = 610 nm, area under the emission peak), the absorbance at the excitation wavelength (610 nm), and the refractive index of the solvent, respectively. Unsubstituted zinc(II) phthalocyanine (ZnPc) in DMF was used as the reference (Φ_F = 0.28). The Φ_F measurements were performed using diluted solutions (absorbances of PSs at 610 nm are 0.04-0.05). Singlet oxygen quantum yields (Φ_Δ) were measured using 1,3-diphenylisobenzofuran (DPBF) as the scavenger. Light laser (670 nm, 80 $mW \cdot cm^{-2}$) was used as the light source and ZnPc was selected as the reference (Φ_Δ = 0.56 in DMF).

***In Vitro* Specificity Studies.** For uptake competition experments, about 7×10^4 MCF-7 cells in 1000 μL DMEM were seeded on a cell culture dish (diameter = 35 mm) and incubated overnight at 37 ℃ under 5% CO_2. MCF-7 cells were incubated with increasing concentrations of 17β-estradiol for 30 h, and subsequently with 0.05 μM conjugate **4** or reference **M** for 24 h. After incubation, the old medium was discarded and the cells were rinsed with PBS for three times, and then the cellular uptake of these phthalocyanines was revealed by comparing the intracellular fluorescence (excited at 633 nm, monitored at 650−750 nm).

For inhibition effects of estrogen on cytotoxicity of conjugate **4** or reference **M**, MCF-7 cells were seeded onto 96-well plates at 3000 cells per well and incubated overnight with increasing concentrations of estrogen (0, 25, 50 μM). After 30 h incubation, the old medium containing estrogen was replaced by fresh medium containing 0.05 μM conjugate **4** or reference **M**. After 24 h incubation, the old medium was discarded and the cells were rinsed with PBS for three times, then the cells were exposed to red light (670 nm) at a dose of 1.5 $J \cdot cm^{-2}$. The cells after irradiation were incubated again for 24 h and then a MTT solution in PBS (10 μL, 4 $mg \cdot mL^{-1}$) was added to each well followed by incubation for 3-4 h. 100 μL DMSO was then added into each well. The plate was incubated at room temperature for 30 min. The absorbance at 570 nm at each well was taken by a microplate reader.

Cellular Uptake. Approximately 3.0×10^4 MCF-7 or MDA-MB-231 cells in 100 μL culture medium (per well) were seeded on 96-multiwell plates and incubated overnight at 37 °C under 5% CO_2. The old culture medium was removed, and then cells were incubated with a solution of phthalocyanine in fresh medium (10 μM, containing 1% DMSO) for 24 h under the same conditions. The solution was then removed, and the cells were rinsed with PBS three times and then lysed by 1% SDS solution to give a homogenous solution. The fluorescence of phthalocyanine in the cell extract was measured on a Bio-Tek microplate reader (λ_{ex} : 610 nm, λ_{em}: 680 nm). Cellular protein content was determined with a BCA Protein Assay Kit (Beyotime Institute of Biotechnology Co., Ltd., China). Results are expressed as nmol photosensitiser per mg cell protein.

***In Vivo* Specificity Studies.** All the animal experiments were approved by the IACUC. Male Balb/c nude mice (4 weeks old, 20–25 g, purchased from Model Animal Research Center of

Nanjing University, Nanjing, China) were maintained and handled in accordance with the recommendations of the institutional animal care and use committee (IACUC). The animals were kept under a pathogen-free condition with free access to sterilised water and food throughout the course of the experiments. The MCF-7 cells (5×10^7 cells in 200 μL) were inoculated subcutaneously into the right flank of the mice. 100 μL estrogen (0.3 mg·mL) were subcutaneously injected near the inoculation site every day. Once the tumors were grown to the size of 100-120 mm^3, the injection of estrogen was stoped and the mice bearing MCF-7 tumors were used for *in vivo* three-dimensional fluorescence imaging. Conjugate **4** and phthalocyanine **M** were dissolved in dimethylacetamide (DMAC) containing 3.8 % cremophor to give 0.5 mM solutions, which were then diluted to appropriate concentrations with PBS (25 μM conjugate **4** or **M**, 4.8% DMAC, 0.19% CEL). Then the final solution of conjugate **4** and phthalocyanine **M** (0.125 μmol/kg of mice body weight) in 100 μL were injected into the mice via tail vein respectively. After injection, mice in each group (the group administrated with conjugate **4** [n = 4], the group administrated with phthalocyanine **M** [n = 2]) were anaesthetized with isoflurane and the tumor targeting capability of the agents within the mice was monitored at different time points (24 h, 48 h, 72 h, 96 h) by using a fluorescent molecular tomography FMT 2500TM LX instrument (PerkinElmer, Waltham, MA, USA) excitated at 680 nm and detected at emission 690–740 nm. For quantitation the average concentrations of the agents, 1 μM conjugate **4** or phthalocyanine **M** diluted by saline was used as a standard to calibrate the instrument. The images were then reconstructed by the software TrueQuant v3.0 (PerkinElmer, USA) to three-dimension models. The quantitative information of drug average concentrations was obtained by creating ROIs around the tumor sites and non-tumor sites after the subtraction of auto-fluorescence from the mice without administration of agents.

***In Vitro* Photodynamic Activities.** MCF-7 cells were seeded onto 96-well plates at 3000 cells per well and incubated overnight. Conjugate **4** or phthalocyanine **M** were diluted to the needed concentration and added to six plicate wells. After 24 h incubation, the old medium containing drugs was replaced by fresh medium and the cells were exposed to red light (λ = 670 nm, 80 mW cm^{-2}, 1.5 J cm^{-2}). The cells after irradiation were incubated again for 24 h and then a MTT solution in PBS (10 μL, 4 $mg{\cdot}mL^{-1}$) was added to each well followed by incubation for 3-4 h. 100 μL DMSO was then added into each well. The plate was incubated at room temperature for 30 min. The absorbance at 570 nm at each well was taken by a microplate reader. For the dark toxicity, the procedures are almost the same as above, except that there is no irradiation. The survival curves were plotted as a function of concentration of dyes and IC_{50} values were calculated.

For dose-dependent photodynamic activities of conjugate **4**, about 7×10^4 MCF-7 cells in 1000 μL DMEM were seeded on a cell culture dish (diameter = 35 mm) and incubated overnight at 37 ℃ under 5% CO_2. Then the cells were treated with different concentration of conjugate **4** (0.005, 0.05, 0.5 μM) for 20 h. The old medium was removed and the cells were rinsed with PBS for three times. Then, the culture medium containing 5 μM calcein AM was added into the cells. After incubation for 40 mins, the intracellular fluorescence of calcein AM was revealed by confocal laser scanning microscopy (ex/em ~488 nm/~520-540 nm).

Intracellular ROS Measurements. Reactive oxygen species (ROS) were measured on the basis of the intracellular peroxide-dependent oxidation of DCFH-DA to form the fluorescent compound 2,7-dichlorofluorescein (DCF). Cells were seeded on to a 96-well plate at a density of 15 000 cells per well and cultured overnight. Then fresh medium containing different

concentration of conjugate **4** (0.001, 0.005, 0.01, 0.05, 0.1, 0.5 μM) was added and cells were incubated for 24 h in dark. After washing three times with PBS, 50 μL DCFH-DA (10 μM) was added and cells were incubated for 30 min. The old medium was discarded and washed three times with PBS followed by illumination for 20 min (light dose of 1.5 $J \cdot cm^{-2}$) with a 96 wells matched-LED light source (670 nm) designed by our lab. Then the cells were lysed with 1% SDS (120 μL) for 10 min at a table concentrator and then the DCF fluorescence was measured by a Bio-Tek microplate reader (excitation/emission: 488/525 nm).

***In Vitro* Antiproliferation Activities in Dark.** MCF-7 cells were seeded onto 96-well plates at 3000 cells per well and incubated overnight. Conjugate **4**, reference **M**, and tamoxifen were diluted to the needed concentration and added to six plicate wells. After 48 h incubation, the old medium containing drugs was replaced by fresh medium, and then a MTT solution in PBS (10 μL, 4 $mg \cdot mL^{-1}$) was added to each well followed by incubation for 3-4 h. 100 μL DMSO was then added into each well. The plate was incubated at room temperature for 30 min. The absorbance at 570 nm at each well was taken by a microplate reader. The survival curves were plotted as a function of concentration of dyes and IC_{50} values were calculated.

About 7×10^4 MCF-7 cells in 1000 μL DMEM were seeded on a cell culture dish (diameter = 35 mm) and incubated overnight at 37 ℃ under 5% CO_2. Then the cells were treated with 25 μM conjugate **4**, reference **M**, and tamoxifen for 48 h. After incubation, the old medium containing drugs was discarded and the cells were rinsed with PBS for three times, and then the culture medium containing 5 μM calcein AM was added and the cells were incubated for 40 mins again, after incubation, the intracellular fluorescence of calcein AM were revealed by confocal laser scanning microscope (ex/em ~488 nm/~520-540 nm).

Subcellular Localisation. Approximately 5×10^4 MCF-7 cells were plated on a cell culture dish (diameter = 35 mm) and incubated overnight. Then the medium was replaced by fresh medium containing 10 μM conjugate **4** and the cells were incubated for 24 h again. After incubation, the cells were rinsed with PBS three times and incubated with MitoTracker Green (Beyotime Institute of Biotechnology Co., Ltd, 2 μM in culture medium, Incubated for 30 min), LysoTracker DND-26 (Xiamen Bioluminor Bio-Technology Co., Ltd, 2 μM in culture medium, Incubated for 30 min) or DAPI (5 min at room temperature). Then the cells were rinsed with PBS three times again and the subcellular localisation of conjugate **4** was revealed by comparing the intracellular fluorescence images caused by the fluorescent probe and phthalocyanines.

ASSOCIATED CONTENT

Supporting Information

Electronic absorption spectra of conjugate **4** and reference **M** in DMEM culture medium, ^{1}H NMR, ^{13}C NMR, HRMS and IR spectra of all the new compounds, and molecular formula strings.

AUTHOR INFORMATION

Corresponding Author

Jian-Yong Liu[*, ξ]: liujianyong82@163.com

Zhi-Hong Zhang,[*, ϖ]: zhangzhh85@126.com

Author Contributions

The manuscript was written through contributions of all authors. All authors have given approval to the final version of the manuscript.

Funding Sources

the National Natural Science Foundation of China (project Nos. 21471033 and 21101028), the Major Project of the State Ministry of Science and Technology of China (project No. 2011ZX09101-001-04), the Key Project of Science and Technology Development of Fujian Province (project No. 2015Y0086), the Independent Research Project of State Key Laboratory of Photocatalysis on Energy and Environment (project Nos. 2014C04 and 2014A04), the School found of Zhejiang Chinese Medical University (project No. 2015ZR07).

Notes

Any additional relevant notes should be placed here.

ACKNOWLEDGMENT

The authors are grateful to the National Natural Science Foundation of China (project Nos. 21471033 and 21101028), the Major Project of the State Ministry of Science and Technology of China (project No. 2011ZX09101-001-04), the Key Project of Science and Technology Development of Fujian Province (project No. 2015Y0086), the Independent Research Project of State Key Laboratory of Photocatalysis on Energy and Environment (project Nos. 2014C04 and 2014A04), the School found of Zhejiang Chinese Medical University (project No. 2015ZR07).

ABBREVIATIONS

ER, estrogen receptors; PDT, Photodynamic therapy; PS, photosensitiser; ROS, reactive oxygen species; E2, 17β-estradiol; SERMs, Specific estrogen receptor modulators; AcE-Cl, α-chloroethyl chloroformate; DBU, 1,8-diazabicyclo[5.4.0]undec-7-ene; Φ_F, fluorescence quantum

yield; Φ_{Δ}, singlet oxygen quantum yield; DPBF, 1, 3-diphenylisobenzofuran; DCFH-DA , 2′, 7′-dichlorodihydrofluorescein diacetate.

REFERENCES

(1) Dolmans, D. E.; Fukumura, D.; Jain, R. K. Photodynamic therapy for cancer. *Nat. Rev. Cancer* **2003**, *3*, 380-387.

(2) Castano, A. P.; Mroz, P.; Hamblin, M. R. Photodynamic therapy and anti-tumour immunity. *Nat. Rev. Cancer* **2006**, *6*, 535-545.

(3) Celli, J. P.; Spring, B. Q.; Rizvi, I.; Evans, C. L.; Samkoe, K. S.; Verma, S.; Pogue, B. W.; Hasan, T. Imaging and photodynamic therapy: mechanisms, monitoring, and optimization. *Chem. Rev.* **2010**, *110*, 2795-2838.

(4) Sharman, W. M.; Allen, C. M.; Van Lier, J. E. Photodynamic therapeutics: basic principles and clinical applications. *Drug Discovery Today* **1999**, *4*, 507-517.

(5) Hah, H. J.; Kim, G.; Lee, Y. E. K.; Orringer, D. A.; Sagher, O.; Philbert, M. A.; Kopelman, R. Methylene blue-conjugated hydrogel nanoparticles and tumor-cell targeted photodynamic therapy. *Macromol. Biosci.* **2011**, *11*, 90-99.

(6) Tian, J.; Ding, L.; Xu, H.-J.; Shen, Z.; Ju, H.; Jia, L.; Bao, L.; Yu, J.-S. Cell-specific and pH-activatable rubyrin-loaded nanoparticles for highly selective near-infrared photodynamic therapy against cancer. *J. Am. Chem. Soc.* **2013**, *135*, 18850-18858.

(7) Zhao, X.; Chen, Z.; Zhao, H.; Zhang, D.; Tao, L.; Lan, M. Multifunctional magnetic nanoparticles for simultaneous cancer near-infrared imaging and targeting photodynamic therapy.

RSC Adv. **2014**, *4*, 62153-62159.

(8) Yu, J.; Hsu, C.-H.; Huang, C.-C.; Chang, P.-Y. Development of therapeutic Au-methylene blue nanoparticles for targeted photodynamic therapy of cervical cancer cells. *ACS Appl. Mater. Interfaces* **2015**, *7*, 432-441.

(9) Park, J.; Jiang, Q.; Feng, D.; Mao, L.; Zhou, H.-C. Size-controlled synthesis of porphyrinic metal-organic framework and functionalization for targeted photodynamic therapy. *J. Am. Chem. Soc.* **2016**, *138*, 3518-3525.

(10) Ma, Z.; Zhang, M.; Jia, X.; Bai, J.; Ruan, Y.; Wang, C.; Sun, X.; Jiang, X. Fe(III)-doped two-dimensional C_3N_4 nanofusiform: a new O_2-evolving and mitochondria-targeting photodynamic agent for MRI and enhanced antitumor therapy. *Small* **2016**, *12*, 5477-5487.

(11) Vrouenraets, M. B.; Visser, G. W.; Stigter, M.; Oppelaar, H.; Snow, G. B.; van Dongen, G. A. Comparison of aluminium (III) phthalocyanine tetrasulfonate-and meta-tetrahydroxyphenylchlorin-monoclonal antibody conjugates for their efficacy in photodynamic therapy in vitro. *Int. J. Cancer* **2002**, *98*, 793-798.

(12) Vrouenraets, M. B.; Visser, G. W.; Stigter, M.; Oppelaar, H.; Snow, G. B.; van Dongen, G. A. Targeting of aluminum (III) phthalocyanine tetrasulfonate by use of internalizing monoclonal antibodies improved efficacy in photodynamic therapy. *Cancer Res.* **2001**, *61*, 1970-1975.

(13) Zhang, C.; Gao, L.; Cai, Y.; Liu, H.; Gao, D.; Lai, J.; Jia, B.; Wang, F.; Liu, Z. Inhibition of tumor growth and metastasis by photoimmunotherapy targeting tumor-associated macrophage in a sorafenib-resistant tumor model. *Biomaterials* **2016**, *84*, 1-12.

(14) Schmidt-Erfurth, U.; Diddens, H.; Birngruber, R.; Hasan, T. Photodynamic targeting of human retinoblastoma cells using covalent low-density lipoprotein conjugates. *Br. J. cancer* **1997**, *75*, 54-61.

(15) Urizzi, P.; Allen, C. M.; Langlois, R.; Ouellet, R.; La Madeleine, C.; Van Lier, J. E. Low-density lipoprotein-bound aluminum sulfophthalocyanine: targeting tumor cells for photodynamic therapy. *J. Porphyrins Phthalocyanines* **2001**, *5*, 154-160.

(16) Chen, Z.; Xu, P.; Chen, J.; Chen, H.; Hu, P.; Chen, X.; Lin, L.; Huang, Y.; Zheng, K.; Zhou, S. Zinc phthalocyanine conjugated with the amino-terminal fragment of urokinase for tumor-targeting photodynamic therapy. *Acta Biomater.* **2014**, *10*, 4257-4268.

(17) Tirand, L.; Frochot, C.; Vanderesse, R.; Thomas, N.; Trinquet, E.; Pinel, S.; Viriot, M.-L.; Guillemin, F.; Barberi-Heyob, M. A peptide competing with VEGF 165 binding on neuropilin-1 mediates targeting of a chlorin-type photosensitizer and potentiates its photodynamic activity in human endothelial cells. *J. Controlled Release* **2006**, *111*, 153-164.

(18) Sibrian-Vazquez, M.; Jensen, T. J.; Vicente, M. G. H. Synthesis, characterization, and metabolic stability of porphyrin-peptide conjugates bearing bifunctional signaling sequences. *J. Med. Chem.* **2008**, *51*, 2915-2923.

(19) Kamarulzaman, E. E.; Gazzali, A. M.; Acherar, S.; Frochot, C.; Barberi-Heyob, M.; Boura, C.; Chaimbault, P.; Sibille, E.; Wahab, H. A.; Vanderesse, R. New peptide-conjugated chlorin-type photosensitizer targeting neuropilin-1 for anti-vascular targeted photodynamic therapy. *Int. J. Mol. Sci.* **2015**, *16*, 24059-24080.

(20) Li, S.-Y.; Cheng, H.; Qiu, W.-X.; Liu, L.-H.; Chen, S.; Hu, Y.; Xie, B.-R.; Li, B.; Zhang,

X.-Z. Protease-activable cell-penetrating peptide-protoporphyrin conjugate for targeted photodynamic therapy in vivo. *ACS Appl. Mater. Interfaces* **2015**, *7*, 28319-28329.

(21) Luan, L.; Fang, W.; Liu, W.; Tian, M.; Ni, Y.; Chen, X.; Yu, X. Phthalocyanine-cRGD conjugate: synthesis, photophysical properties and in vitro biological activity for targeting photodynamic therapy. *Org. Biomol. Chem.* **2016**, *14*, 2985-2992.

(22) Hamblin, M. R.; Newman, E. L. Photosensitizer targeting in photodynamic therapy I. Conjugates of haematoporphyrin with albumin and transferrin. *J. Photochem. Photobiol., B* **1994**, *26*, 45-56.

(23) Cavanaugh, P. G. Synthesis of chlorin e6-transferrin and demonstration of its light-dependent in vitro breast cancer cell killing ability. *Breast Cancer Res. Treat.* **2002**, *72*, 117-130.

(24) Gao, Y.; Qiao, G.; Zhuo, L.; Li, N.; Liu, Y.; Tang, B. A tumor mRNA-mediated bi-photosensitizer molecular beacon as an efficient imaging and photosensitizing agent. *Chem. Commun.* **2011**, *47*, 5316-5318.

(25) Mallikaratchy, P.; Tang, Z.; Tan, W. Cell specific aptamer-photosensitizer conjugates as a molecular tool in photodynamic therapy. *ChemMedChem* **2008**, *3*, 425-428.

(26) Schneider, R.; Schmitt, F.; Frochot, C.; Fort, Y.; Lourette, N.; Guillemin, F.; Müller, J. F.; Barberi-Heyob, M. Design, synthesis, and biological evaluation of folic acid targeted tetraphenylporphyrin as novel photosensitizers for selective photodynamic therapy. *Bioorg. Med. Chem.* **2005**, *13*, 2799-2808.

(27) Ke, M.-R.; Yeung, S.-L.; Ng, D. K.; Fong, W.-P.; Lo, P.-C. Preparation and in vitro

photodynamic activities of folate-conjugated distyryl boron dipyrromethene based photosensitizers. *J. Med. Chem.* **2013**, *56*, 8475-8483.

(28) Stallivieri, A.; Colombeau, L.; Jetpisbayeva, G.; Moussaron, A.; Myrzakhmetov, B.; Arnoux, P.; Acherar, S.; Vanderesse, R.; Frochot, C. Folic acid conjugates with photosensitizers for cancer targeting in photodynamic therapy: synthesis and photophysical properties. *Bioorg. Med. Chem.* **2017**, *25*, 1-10.

(29) Göksel, M. Synthesis of asymmetric zinc (II) phthalocyanines with two different functional groups & spectroscopic properties and photodynamic activity for photodynamic therapy. *Bioorg. Med. Chem.* **2016**, *24*, 4152-4164.

(30) Shin, W. S.; Han, J.; Kumar, R.; Lee, G. G.; Sessler, J. L.; Kim, J.-H.; Kim, J. S. Programmed activation of cancer cell apoptosis: a tumor-targeted phototherapeutic topoisomerase I inhibitor. *Sci. Rep.* **2016**, *6*, 29018.

(31) Yin Zhang, K.; Ka-Shun Tso, K.; Louie, M.-W.; Liu, H.-W.; Kam-Wing Lo, K. A phosphorescent rhenium (I) tricarbonyl polypyridine complex appended with a fructose pendant that exhibits photocytotoxicity and enhanced uptake by breast cancer cells. *Organometallics* **2013**, *32*, 5098-5102.

(32) Singh, S.; Aggarwal, A.; Bhupathiraju, N. D. K.; Tiwari, K.; Drain, C. M. Glycosylated porphyrins, phthalocyanines, and other porphyrinoids for diagnostics and therapeutics. *Chem. Rev.* 2**015**, *115*, 10261-10306.

(33) Shivran, N.; Tyagi, M.; Mula, S.; Gupta, P.; Saha, B.; Patro, B. S.; Chattopadhyay, S. Synthesis and photodynamic activity of some glucose-conjugated BODIPY dyes. *Eur. J. Med.*

Chem. **2016**, *122*, 352-365.

(34) Zuluaga, M.-F.; Lange, N. Combination of photodynamic therapy with anti-cancer agents. *Curr. Med. Chem.* **2008**, *15*, 1655-1673.

(35) Khdair, A.; Handa, H.; Mao, G.; Panyam, J. Nanoparticle-mediated combination chemotherapy and photodynamic therapy overcomes tumor drug resistance in vitro. *Eur. J. Pharm. Biopharm.* **2009**, *71*, 214-222.

(36) Kaiser, P. K. Verteporfin photodynamic therapy combined with intravitreal bevacizumab for neovascular age-related macular degeneration. *Ophthalmology* **2009**, *116*, 747-755.

(37) Mao, J.; Zhang, Y.; Zhu, J.; Zhang, C.; Guo, Z. Molecular combo of photodynamic therapeutic agent silicon (IV) phthalocyanine and anticancer drug cisplatin. *Chem. Commun.* **2009**, *45*, 908-910.

(38) Mennel, S.; Meyer, C. H.; Callizo, J. Combined intravitreal anti-vascular endothelial growth factor (Avastin®) and photodynamic therapy to treat retinal juxtapapillary capillary haemangioma. *Acta Ophthalmol.* **2010**. *88*, 610-613.

(39) Rizvi, I.; Celli, J. P.; Evans, C. L.; Abu-Yousif, A. O.; Muzikansky, A.; Pogue, B. W.; Finkelstein, D.; Hasan, T. Synergistic enhancement of carboplatin efficacy with photodynamic therapy in a three-dimensional model for micrometastatic ovarian cancer. *Cancer Res.* **2010**, *70*, 9319-9328.

(40) Lau, J. T.; Lo, P.-C.; Fong, W.-P.; Ng, D. K. A zinc (II) phthalocyanine conjugated with an oxaliplatin derivative for dual chemo-and photodynamic therapy. *J. Med. Chem.* **2012**, *55*, 5446-

5454.

(41) Zhang, F.-L.; Huang, Q.; Zheng, K.; Li, J.; Liu, J.-Y.; Xue, J.-P. A novel strategy for targeting photodynamic therapy. Molecular combo of photodynamic agent zinc (II) phthalocyanine and small molecule target-based anticancer drug erlotinib. *Chem. Commun.* **2013**, *49*, 9570-9572.

(42) Zhou, X. Q.; Meng, L. B.; Huang, Q.; Li, J.; Zheng, K.; Zhang, F. L.; Liu, J. Y.; Xue, J. P. Synthesis and in vitro anticancer activity of zinc (II) phthalocyanines conjugated with coumarin derivatives for dual photodynamic and chemotherapy. *ChemMedChem* **2015**, *10*, 304-311.

(43) Zhang, F. L.; Huang, Q.; Liu, J. Y.; Huang, M. D.; Xue, J. P. Molecular-target-based anticancer photosensitizer: synthesis and in vitro photodynamic activity of erlotinib-zinc (II) phthalocyanine conjugates. *ChemMedChem* **2015**, *10*, 312-320.

(44) Bio, M.; Rajaputra, P.; Nkepang, G.; Awuah, S. G.; Hossion, A. M.; You, Y. Site-specific and far-red-light-activatable prodrug of combretastatin A-4 using photo-unclick chemistry. *J. Med. Chem.* **2013**, *56*, 3936-3942.

(45) Bio, M.; Rajaputra, P.; Nkepang, G.; You, Y. Far-red light activatable, multifunctional prodrug for fluorescence optical imaging and combinational treatment. *J. Med. Chem.* **2014**, *57*, 3401-3409.

(46) Rajaputra, P.; Bio, M.; Nkepang, G.; Thapa, P.; Woo, S.; You, Y. Anticancer drug released from near IR-activated prodrug overcomes spatiotemporal limits of singlet oxygen. *Bioorg. Med. Chem.* **2016**, *24*, 1540-1549.

(47) Thapa, P.; Li, M.; Bio, M.; Rajaputra, P.; Nkepang, G.; Sun, Y.; Woo, S.; You, Y. Far-red light-activatable prodrug of paclitaxel for the combined effects of photodynamic therapy and site-specific paclitaxel chemotherapy. *J. Med. Chem.* **2016**, *59*, 3204-3214.

(48) Liu, L. H.; Qiu, W. X.; Li, B.; Zhang, C.; Sun, L. F.; Wan, S. S.; Rong, L.; Zhang, X. Z. A red light activatable multifunctional prodrug for image-guided photodynamic therapy and cascaded chemotherapy. *Adv. Funct. Mater.* **2016**, *26*, 6257-6269.

(49) Yuan, Y.; Liu, J.; Liu, B. Conjugated-polyelectrolyte-based polyprodrug: targeted and image-guided photodynamic and chemotherapy with on-demand drug release upon irradiation with a single light source. *Angew. Chem. Int. Ed.* **2014**, *53*, 7163-7168.

(50) Li, H.; Li, Z.; Liu, L.; Lu, T.; Wang, Y. An efficient gold nanocarrier for combined chemo-photodynamic therapy on tumour cells. *RSC Adv.* **2015**, *5*, 34831-34838.

(51) He, C.; Liu, D.; Lin, W. Self-assembled core-shell nanoparticles for combined chemotherapy and photodynamic therapy of resistant head and neck cancers. *ACS Nano* **2015**, *9*, 991-1003.

(52) Chen, C. Y.; Syu, C. K.; Lin, H. C. A stimulated mixed micelle system for in vitro study on chemo-photodynamic therapy. *Macromol. Biosci.* **2016**, *16*, 188-197.

(53) Obrero, M.; David, V. Y.; Shapiro, D. J. Estrogen receptor-dependent and estrogen receptor-independent pathways for tamoxifen and 4-hydroxytamoxifen-induced programmed cell death. *J. Biol. Chem.* **2002**, *277*, 45695-45703.

(54) Grate J. W.; Frye G. C. In *Sensors Update*, Vol. 2.; Baltes, H., Göpel, W., Hesse, J., Eds.;

Wiley-VCH: Weinheim, 1996; pp 10-20.

(55) Jordan, V. C. Chemoprevention of breast cancer with selective oestrogen-receptor modulators. *Nat. Rev. Cancer* **2007**, *7*, 46-53.

(56) Shiau, A. K.; Barstad, D.; Loria, P. M.; Cheng, L.; Kushner, P. J.; Agard, D. A.; Greene, G. L. The structural basis of estrogen receptor/coactivator recognition and the antagonism of this interaction by tamoxifen. *Cell* **1998**, *95*, 927-937.

(57) Coezy, E.; Borgna, J.-L.; Rochefort, H. Tamoxifen and metabolites in MCF7 cells: correlation between binding to estrogen receptor and inhibition of cell growth. *Cancer Res.* **1982**, *42*, 317-323.

(58) Jordan, V. C. Tamoxifen: a most unlikely pioneering medicine. *Nat. Rev. Drug Discovery* **2003**, *2*, 205-213.

(59) Khan, E. H.; Ali, H.; Tian, H.; Rousseau, J.; Tessier, G.; van Lier, J. E. Synthesis and biological activities of phthalocyanine-estradiol conjugates. *Bioorg. Med. Chem. Lett.* **2003**, *13*, 1287-1290.

(60) Swamy, N.; Purohit, A.; Fernandez-Gacio, A.; Jones, G. B.; Ray, R. Nuclear estrogen receptor targeted photodynamic therapy: selective uptake and killing of MCF-7 breast cancer cells by a C17α-alkynylestradiol-porphyrin conjugate. *J. Cell. Biochem.* **2006**, *99*, 966-977.

(61) Novakova, V.; Zimcik, P.; Miletin, M.; Kopecky, K.; Ivincová, J. A phthalocyanine-mestranol conjugate for photodynamic therapy prepared via click chemistry. *Tetrahedron Lett.* **2010**, *51*, 1016-1018.

(62) Gacio, A. F.; Fernandez-Marcos, C.; Swamy, N.; Dunn, D.; Ray, R. Photodynamic cell-kill analysis of breast tumor cells with a tamoxifen-pyropheophorbide conjugate. *J. Cell. Biochem.* **2006**, *99*, 665-670.

(63) Olofson, R.; Martz, J. T.; Senet, J. P.; Piteau, M.; Malfroot, T. A new reagent for the selective, high-yield N-dealkylation of tertiary amines: improved syntheses of naltrexone and nalbuphine. *J. Org. Chem.* **1984**, *49*, 2081-2082.

(64) Dreaden, E. C.; Mwakwari, S. C.; Sodji, Q. H.; Oyelere, A. K.; El-Sayed, M. A. Tamoxifen-poly (ethylene glycol)-thiol gold nanoparticle conjugates: enhanced potency and selective delivery for breast cancer treatment. *Bioconjugate Chem.* **2009**, *20*, 2247-2253.

(65) Scalise, I.; Durantini, E. N. Synthesis, properties, and photodynamic inactivation of Escherichia coli using a cationic and a noncharged Zn (II) pyridyloxyphthalocyanine derivatives. *Bioorg. Med. Chem.* **2005**, *13*, 3037-3045.

(66) Maree, M. D.; Kuznetsova, N.; Nyokong, T. Silicon octaphenoxyphthalocyanines: photostability and singlet oxygen quantum yields. *J. Photochem. Photobiol., A* **2001**, *140*, 117-125.

(67) Rich, R. L.; Hoth, L. R.; Geoghegan, K. F.; Brown, T. A.; LeMotte, P. K.; Simons, S. P.; Hensley, P.; Myszka, D. G. Kinetic analysis of estrogen receptor/ligand interactions. *Proc. Natl. Acad. Sci. U. S. A*, **2002**, *99*, 8562-8567.

(68) Decherchi, P.; Cochard, P.; Gauthier, P. Dual staining assessment of Schwann cell viability within whole peripheral nerves using calcein-AM and ethidium homodimer. *J. Neurosci. Methods* **1997**, *71*, 205-213.

(69) Snow, A. In *The Porphyrin Handbook*, Vol. 17; Kadish, K.M., Smith, K.M., Guilard, R., eds.; Academic Press: San Diego, 2003; pp 129-176.

Table of contents entry